Fluctuations and correlations of conserved charges in an excluded-volume hadron resonance gas model

Abhijit Bhattacharyya*
Department of Physics, University of Calcutta, 92, A.P.C. Road, Kolkata 700009, India

Supriya Das,† Sanjay K. Ghosh,‡ Rajarshi Ray,§ and Subhasis Samanta‖
Center for Astroparticle Physics & Space Science, Bose Institute, Block EN, Sector V, Salt Lake, Kolkata 700091, India
and Department of Physics, Bose Institute, 93/1, A.P.C. Road, Kolkata 700009, India
(Received 21 October 2013; revised manuscript received 30 July 2014; published 17 September 2014)

We present temperature and baryonic chemical potential dependence of higher-order fluctuations and the correlation between conserved charges in an excluded-volume hadron resonance gas model. Products of moments, such as the ratio of variance to mean, product of skewness and standard deviation, product of kurtosis and variance, for the net proton, net kaon, and net charge have been evaluated on the phenomenologically determined freeze-out curve. Further, products of moments for net proton and net charge have been compared with the experimental data measured by the STAR experiment. The dependence of the model result on the hadronic radius parameter has also been discussed.

DOI: 10.1103/PhysRevC.90.034909 PACS number(s): 21.65.Mn, 12.38.Mh, 21.60.−n

I. INTRODUCTION

One of the primary goals of heavy-ion collision experiments at ultrarelativistic energies is to study the thermodynamic aspects of strongly interacting matter at high temperature and density. While at low density and high temperature, present experimental as well as lattice data seem to indicate a smooth crossover [1,2] from hadronic to a quark gluon matter, at high density and low temperature the system is expected to have a first-order transition [3–8]. So the first-order phase transition at high densities and low temperature should end at a critical end point (CEP)—a second-order phase transition point—as one moves towards a high-temperature and low-density region, in the phase diagram of strongly interacting matter [9–12].

Several experimental programs have been launched to study the phase transition of strongly interacting matter. At present, the Relativistic Heavy-Ion Collider (RHIC) at Brookhaven National Laboratory and the Large Hadron Collider (LHC) at CERN are providing us a plethora of data. In the near future the Facility for Anti-proton and Ion Research (FAIR) at GSI will also provide us a large amount of information. The low-temperature and high baryonic chemical potential (μ_B) region will be studied in the Beam Energy Scan (BES) program of RHIC and the Compressed Baryonic Matter (CBM) program at FAIR. Those experiments would also explore the first-order line of the phase diagram along with the location of the CEP.

The unveiling of the nature of phase transition requires a proper understanding of quantum chromodynamics (QCD), the theory of strong interactions. Unfortunately, the nonperturbative nature of the phenomena inhibits the use of first-principles QCD for the study of strongly interacting matter at extreme conditions. In this regard lattice QCD (LQCD) provides the most direct approach to study QCD at high temperature [1,13–27]. However LQCD has its own restrictions due to the discretization of space time. Furthermore, at finite chemical potential, LQCD faces the well-known sign problem.

In contrast, effective models [28–30] provide a simpler alternative for the study of the strongly interacting matter in the nonperturbative domain. Some of these models have been quite successful in describing the physics of strongly interacting matter. For example, the Polyakov loop extended Nambu-Jona-Lasinio model (PNJL) has been used to study various aspects of the physics of strongly interacting matter at high temperatures and was found to reproduce the zero density lattice data quite successfully [28,29]. On the other hand, the hadron resonance gas (HRG) model [31] has been very successful in describing the hadron yields in central heavy-ion collisions from AGS up to RHIC energies [32–39].

A reliable way to understand the physics of the phase transition of strongly interacting matter is to study the correlations and fluctuations of conserved charges. Susceptibilities are related to fluctuations via the fluctuation-dissipation theorem. A measure of the intrinsic statistical fluctuations in a system close to thermal equilibrium is provided by the corresponding susceptibilities. At finite temperature and chemical potential fluctuations of conserved charges are sensitive indicators of the transition from hadronic matter to quark-gluon plasma (QGP). Moreover, the existence of the CEP can be signaled by the divergent fluctuations. For the small net baryon number, which can be met at different experiments, the transition from hadronic to QGP phase is continuous and the fluctuations are not expected to lead to any singular behavior. Computations on the lattice have been performed for many of these susceptibilities at zero chemical potentials [40–43]. It has been shown that at vanishing chemical potential the susceptibilities rise rapidly around the continuous crossover transition region.

*abphy@caluniv.ac.in
†supriya@jcbose.ac.in
‡sanjay@jcbose.ac.in
§rajarshi@jcbose.ac.in
‖samanta@jcbose.ac.in

Since the prediction of the HRG model for the system at freeze out is in very good agreement with the experiments, it would be interesting to study the susceptibilities as well as higher moments using this model and its interacting version, i.e., the excluded-volume hadron resonance gas (EVHRG) model [44–54]. In fact as the higher moments are expected to be more sensitive to the phase transition, any deviation of experimental observation from the model results may be taken as an indication of new phenomena.

The HRG model is based on the Dashen, Ma, and Bernstein theorem [55], which shows that a dilute system of strongly interacting matter can be described by a gas of free resonances. The attractive part of the hadron interactions is taken care of by these resonances. On the other hand, both the long-range attraction as well as the short-range repulsion are important for the description of strongly interacting matter [52]. Moreover, near critical temperature HRG calculations tends towards Hagedorn divergence, which may be due to the absence of repulsive interaction [50]. This repulsive part is incorporated through the excluded-volume effects in the HRG [45] and is commonly known as the EVHRG model. The EVHRG equations of state have also been used for the hydrodynamical models of nucleus-nucleus collision [56–58]. In the present work we will be discussing our results of susceptibilities and correlations using the EVHRG model.

Recently fluctuations of conserved charges, using the HRG model, have been studied in Ref. [59] where actual experimental acceptances in terms of pseudorapidity and transverse momentum are considered. In Ref. [53], higher moments of net-proton multiplicity have been studied using the EVHRG model.

Our aim in the present work is twofold. First we would like to have a physical understanding of the EVHRG model results *vis-à-vis* HRG, lattice and experimental data. Second, we would like to study the high-density sector to be explored in the beam energy scan at RHIC and the CBM experiment at FAIR.

Here we present the temperature (T) and baryonic chemical potential (μ_B) dependence of susceptibilities of different conserved quantities such as net-baryon number, net strangeness, and net charge up to order four using the EVHRG model. Baryon-strangeness and charge-strangeness correlation functions have been evaluated at different T and μ_B. Different values of baryon and meson radii have been used to study their effect on susceptibilities and correlations. We have discussed experimental observables in the framework of HRG as well as EVHRG models. The product of moments of distribution of conserved quantities are related to the ratio of different order of susceptibilities [60–62] such as $\sigma^2/M = \chi^2/\chi^1$, $S\sigma = \chi^3/\chi^2$ and $\kappa\sigma^2 = \chi^4/\chi^2$ where M is the mean, σ is the standard deviation, S is the skewness, κ is the kurtosis of the distribution of conserved quantities, and χ^n are the nth-order susceptibilities. In general, higher-order susceptibilities are more sensitive to the large correlation length and hence the critical point [30]. This implies that any memory of the large correlation length retained in the thermal system at freeze out would be reflected in the behavior of higher moments. We have studied the energy dependence of product of moments for net proton, net kaon, and net charge and compare our result for net proton and net charge with experimental data of fluctuation along with the transverse momentum and pseudorapidity acceptance.

The paper is organized as follows. The HRG model and its extension to EVHRG are introduced in Sec. II. In Sec. III we have first discussed the fluctuations of different conserved charges and correlations among them at zero μ_B (finite T) and compared them with the lattice data. Then we have discussed the finite density scenario along with a comparison with the experimental data. Finally we have summarized our results in Sec. IV.

II. HADRON RESONANCE GAS MODEL

In this section we are going to discuss the HRG and EVHRG model very briefly. The detailed discussions can be found in Refs. [31–39,44–48,50]. The grand canonical partition function of a hadron resonance gas [31,50] can be written as

$$\ln Z^{id} = \sum_i \ln Z_i^{id}, \tag{1}$$

where the sum is over all the hadrons. id refers to ideal, i.e., noninteracting HRG. For particle i,

$$\ln Z_i^{id} = \pm\frac{V g_i}{2\pi^2}\int_0^\infty p^2\,dp\,\ln\{1 \pm \exp[-(E_i-\mu_i)/T]\}, \tag{2}$$

where V is the volume of the system, g_i is the degeneracy factor, T is the temperature, $E_i = \sqrt{p^2+m_i^2}$ is the single-particle energy, m_i is the mass, and $\mu_i = B_i\mu_B + S_i\mu_S + Q_i\mu_Q$ is the chemical potential. B_i, S_i, Q_i are, respectively, the baryon number, strangeness, and charge of the particle, μ's are corresponding chemical potentials. The (+) and (−) sign corresponds to fermions and bosons respectively. Partition function depends in general on five parameters. However, only three are independent, since μ_Q and μ_S can be found from conservation of different quantum numbers like baryon number, charge and strangeness [31,50].

The partition function is the basic quantity from which one can calculate various thermodynamic quantities of the thermal system created in heavy-ion collisions. The partial pressure P_i, the particle density n_i, the energy density ε_i, and the entropy density s_i can be calculated using the standard definitions,

$$P_i^{id} = \frac{T}{V}\ln Z_i^{id} = \pm\frac{g_i T}{2\pi^2}\int_0^\infty p^2\,dp\,\ln\{1 \pm \exp[-(E_i-\mu_i)/T]\}, \tag{3}$$

$$n_i^{id} = \frac{T}{V}\left(\frac{\partial \ln Z_i^{id}}{\partial\mu_i}\right)_{V,T} = \frac{g_i}{2\pi^2}\int_0^\infty \frac{p^2\,dp}{\exp[(E_i-\mu_i)/T]\pm 1}, \tag{4}$$

$$\varepsilon_i^{id} = \frac{E_i^{id}}{V} = -\frac{1}{V}\left(\frac{\partial \ln Z_i^{id}}{\partial\frac{1}{T}}\right)_{\frac{\mu}{T}} = \frac{g_i}{2\pi^2}\int_0^\infty \frac{p^2\,dp}{\exp[(E_i-\mu_i)/T]\pm 1}E_i, \tag{5}$$

$$s_i^{id} = \frac{S_i^{id}}{V} = \frac{1}{V}\left(\frac{\partial\left(T \ln Z_i^{id}\right)}{\partial T}\right)_{V,\mu}$$
$$= \pm\frac{g_i}{2\pi^2}\int_0^\infty p^2\,dp\left[\ln\left(1 \pm \exp\left(-\frac{(E_i-\mu_i)}{T}\right)\right) \pm \frac{(E_i-\mu_i)}{T\{\exp[(E_i-\mu_i)/T] \pm 1\}}\right]. \quad (6)$$

Since Eqs. (3)–(6) determine the thermodynamic properties of the system, those are called equations of state (EOS) of the system.

Let us now discuss the interacting HRG or EVHRG model. In contrast to the pointlike hadrons in HRG, in the EVHRG model, hadronic phase is modeled by a gas of interacting hadrons, where the geometrical size of the hadrons are explicitly incorporated as the excluded volume correction [45,46,48] to approximate the short-range repulsive hadron-hadron interaction.

Excluded-volume corrections were first introduced in Ref. [44] but it was thermodynamically inconsistent. A thermodynamically consistent excluded volume correction was first proposed in Ref. [45].

In EVHRG model pressure can be written as

$$P(T,\mu_1,\mu_2,\ldots) = \sum_i P_i^{id}(T,\hat{\mu}_1,\hat{\mu}_2,\ldots), \quad (7)$$

where for ith particle the chemical potential is

$$\hat{\mu}_i = \mu_i - V_{ev,i}P(T,\mu_1,\mu_2,\ldots) \quad (8)$$

where $V_{ev,i} = 4\,\frac{4}{3}\,\pi R_i^3$ is the volume excluded for the ith hadron with hard-core radius R_i.

In an iterative procedure one can get the total pressure. Pressure $P(T,\mu_1,\mu_2,\ldots)$ is suppressed compared to the ideal gas pressure P^{id} because of the smaller value of effective chemical potential. The other thermodynamic quantities such as n_i, s, ε can be calculated from Eqs. (7)–(8) as

$$n_i = n_i(T,\mu_1,\mu_2,\ldots) = \frac{\partial P}{\partial \mu_i} = \frac{n_i^{id}(T,\hat{\mu}_i)}{1+\sum_k V_{ev,k}n_k^{id}(T,\hat{\mu}_k)}, \quad (9)$$

$$s = s(T,\mu_1,\mu_2,\ldots) = \left(\frac{\partial P}{\partial T}\right)_{\mu_1,\mu_2,..} = \frac{\sum_i s_i^{id}(T,\hat{\mu}_i)}{1+\sum_k V_{ev,k}n_k^{id}(T,\hat{\mu}_k)}, \quad (10)$$

$$\varepsilon = \varepsilon(T,\mu_1,\mu_2,\ldots) = \frac{\sum_i \varepsilon_i^{id}(T,\hat{\mu}_i)}{1+\sum_k V_{ev,k}n_k^{id}(T,\hat{\mu}_k)}. \quad (11)$$

This correction scheme is thermodynamically consistent, i.e., EOS after corrections obey the relation

$$s = \frac{\varepsilon + P - \sum_i \mu_i n_i}{T}. \quad (12)$$

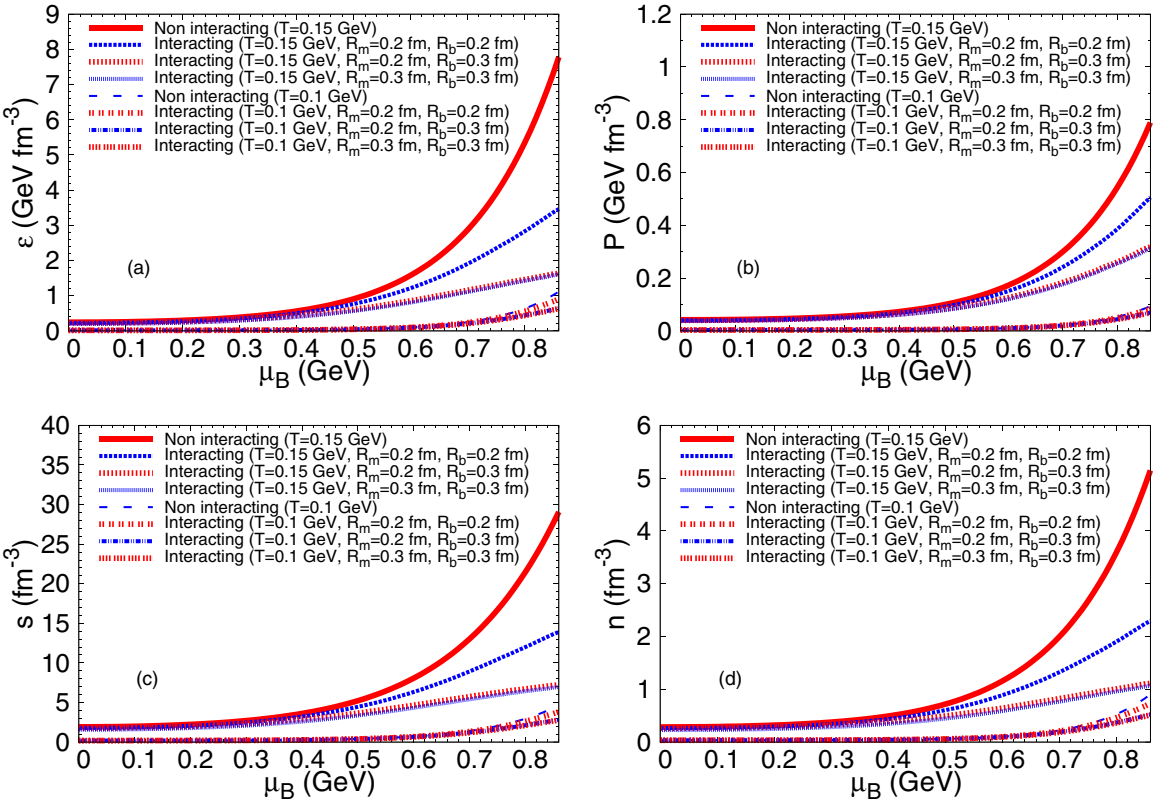

FIG. 1. (Color online) Equations of state as a function of μ_B at constant T keeping $\mu_S = \mu_Q = 0$. Noninteracting means noninteracting HRG model, i.e., without excluded-volume correction, and interacting refers to EVHRG. R_m refers to radius of mesons and R_b refers to radius of baryons.

In this work we have incorporated all the hadrons listed in the particle data book [63] up to mass of 3 GeV. In Fig. 1 we have shown ε, P, s, and n as a function of μ_B at fixed T. For completeness one should also plot these quantities as a function of T at fixed μ_B. However such relations are already given in Refs. [50,54] and we do not repeat those here. Our results show that there is almost no effect of interaction till $\mu_B = 0.4$ GeV in EOS. Beyond $\mu_B = 0.4$ GeV we see quite a substantial change in these quantities. The change is more pronounced at higher temperatures. One can see from this figure that at large μ_B the energy, entropy, and number density in EVHRG model are suppressed by a factor of 2, compared to HRG, if we take the radii of all the hadrons to be 0.2 fm. This is expected as the finite radius acts as repulsive interaction between hadrons. If we increase the size of the baryons further to 0.3 fm the suppression is even more. However the thermodynamic quantities are less sensitive to the mesonic radii as can be seen from Fig. 1. The plot for $R_b = R_m = 0.3$ fm is almost same as that for $R_b = 0.3$ fm, $R_m = 0.2$ fm and is suppressed compared to $R_b = R_m = 0.2$ fm. This is an expected result as the system is dominated by baryons at high μ_B.

The difference of the EVHRG model, as compared to HRG, is governed by the radius parameter. The electromagnetic charge radii of hadrons have been measured by different groups [64]. For example, the radii for p, Σ^-, π^-, and K^- are around 0.8 fm, 0.9 fm, 0.7 fm, and 0.6 fm respectively. One can also define a strong interaction radii [65], which comes out to be around the same values. In accordance with these results, a value of 0.8 fm for baryons and 0.62 fm for mesons were proposed earlier [48]. On the other hand, Braun-Munzinger *et al.* [34] argued that a more realistic approach is to incorporate repulsive behavior of the NN potential using hard-core radius (~ 0.3 fm) as obtained from nucleon-nucleon scattering [66]. The corresponding meson radius should not exceed that of baryons. A similar hard-core radius of 0.2–0.3 fm has also been proposed in Ref. [67] to explain the proton-proton scattering data. It has also been shown earlier that to justify a hydrodynamic approach to heavy-ion collisions within the hadron phase the hard-core hadron radius should be $r \geqslant 0.2$ fm in the EVHRG model [49]. In the present study we have taken an approach similar to Ref. [34] and have used different baryon (R_b) and meson (R_m) radii between 0.2–0.3 fm.

III. FLUCTUATION AND CORRELATION: LATTICE VERSUS EVHRG

Fluctuations and correlations of conserved charges such as net electric charge, baryon number, and strangeness have been considered as probes of hadronization and thermalization of the system created in nuclear collisions [68–70]. Fluctuations are considered to be important signatures for the existence of CEP on the phase diagram as it would lead to large fluctuations in the thermodynamic quantities. Moreover, fluctuations are expected to show distinctly different behavior in a hadron resonance gas and a QGP.

A. Fluctuations of conserved charges

Derivatives of the grand canonical partition function (Z) with respect to chemical potential define susceptibilities, which experimentally become accessible through event-by-event analysis of fluctuations in observable quantities such as baryon number, electric charge, strangeness, and others.

The nth-order susceptibility is defined as

$$\chi_x^n = \frac{1}{VT^3}\frac{\partial^n(lnZ)}{\partial\left(\frac{\mu_x}{T}\right)^n}, \tag{13}$$

where μ_x is the chemical potential for conserved charge x. For our purpose $x = B$ (baryon), S (strangeness), and Q (electric charge).

In Fig. 2 we have shown temperature dependence of pressure and second-order susceptibilities for various conserved charges at zero chemical potentials ($\mu_B = \mu_S = \mu_Q = 0$). From Fig. 2(a), where we plot pressure as a function of temperature, one can see that the continuum limit lattice data from Refs. [25,71] agrees within an error bar with the HRG and EVHRG model up to $T \sim 0.17$ GeV. The second-order susceptibilities are found to increase rapidly with increase of temperature. Near $T = 0.1$ GeV magnitude of χ_Q^2 is almost double compared to χ_S^2 and the magnitude of χ_B^2 is almost zero at this temperature. As at low-temperature, fluctuations of a particular charge are dominated by lightest hadrons carrying that charge. The dominant contribution to χ_B^2 at low temperatures comes from protons (lightest baryon), while χ_S^2 receives leading contribution from kaons (lightest strange hadron) and χ_Q^2 from pions (lightest charged hadron). Since a pion is lighter compared to a proton and kaon, magnitude of χ_Q^2 is more than that of χ_B^2 and χ_S^2. In EVHRG we have considered different values of R_b and R_m as shown in Fig. 2. It can be seen that there is almost no effect of interaction till $T = 0.13$ GeV in fluctuations. The reason for this is that the effective degree of freedom does not increase much up to this temperature and therefore correction due to excluded volume is small. Above $T = 0.13$ GeV we find quite a substantial change in second-order susceptibilities. It can be seen from this figure that at large T, second-order fluctuations are reduced by almost 30% compared to the noninteracting hadrons, if we take radii of all the hadrons to be 0.2 fm. If we increase radii of hadrons further to 0.3 fm, the suppression is even more. We have compared our result with LQCD data [24,27]. It can be seen that up to $T = 0.18$ GeV, χ_B^2 is in good agreement with LQCD if we consider radii of all hadrons to be 0.2 fm whereas χ_Q^2 is in good agreement with LQCD for $R_m = 0.2$ fm and $R_b = 0.3$ fm. The meson radius plays an important role for χ_S^2 and χ_Q^2 but not for χ_B^2, which can be seen from the figure. This is an expected result since in χ_S^2 and χ_Q^2 both the baryons and mesons contribute whereas in χ_B^2 only baryons contribute. One should, however, note that the dependence of χ_B^2 on R_m is not completely negligible. We will address this issue later.

In the noninteracting HRG model, under Boltzmann approximation, $\chi_B^4 \approx \chi_B^2$ and $\chi_B^1 \approx \chi_B^3$ as only baryons with baryon number one contribute to various susceptibilities [61]. In contrast, in the case of higher-order susceptibilities, electric charge and strangeness are expected to show larger values as hadrons with multiple charge/strangeness get larger weight. A similar behavior is expected for the EVRHG model as well. In Fig. 3 we have shown variation of fourth-order susceptibilities with temperature at $\mu = 0$. The nature of all

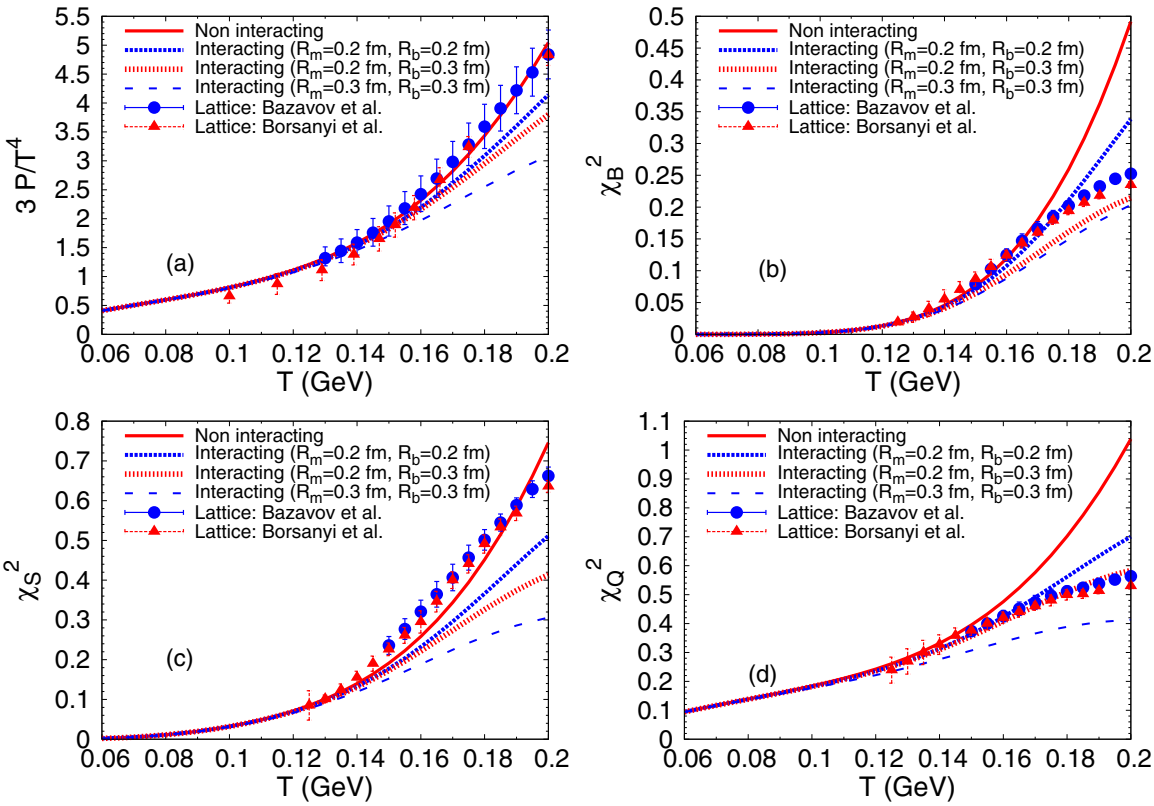

FIG. 2. (Color online) Variation of pressure and second-order susceptibilities χ_B^2, χ_S^2, and χ_Q^2 with temperature at $\mu = 0$. Lattice data for pressure are taken from Bazavov *et al.* [71] and Borsányi *et al.* [25] whereas those for χ^2 are taken from Bazavov *et al.* [24] and Borsányi *et al.* [27].

the fourth-order susceptibilities is similar to second-order susceptibilities. As expected, magnitudes of fourth-order susceptibilities are larger compared to that of second-order susceptibilities for strangeness and electric charge. However this is not true for baryon number fluctuations. Although contributions in χ_B are only from baryons, these quantities also depend on the size of mesons as can be seen from Figs. 2(b) and 3(a). This dependence can be understood from Eqs. (7) and (8), which shows the dependence of chemical potential on hadronic radii through pressure. Hence, even for baryon number susceptibilities there may be small difference in magnitudes of susceptibilities at different R_m for EVHRG. We compare our result with LQCD data ($N_\tau = 6,8$) [72]. The LQCD data for χ_B^4 and χ_S^4 are in good agreement with the HRG model up to $T = 0.16$ GeV. Whereas for χ_Q^4, LQCD data is lower compared to both HRG and EVHRG.

It has been argued in Ref. [50] that for ϵ, P, and s, though lattice QCD results agree at lower temperatures, they are expected to becomes larger than those in HRG at higher temperatures due to deconfinement. On the other hand, the difference between lattice and HRG for the higher susceptibilities may have effects due to the difference in hadronic masses. It has also been reported that the thermodynamic quantities calculated in lattice QCD may agree well with the HRG model if the masses of the hadrons in the model are tuned appropriately to take into account the discretization errors in the hadron spectrum present in the lattice calculations [73,74]. In the present study EVHRG is found to show a better agreement with the lattice data in the continuum limit.

B. Correlations among different conserved charges

Correlations among different conserved charges may act as probes of the structure of QCD at finite temperature. In QGP, as baryon number as well as electric charge are carried by different flavors of quarks, a strong correlation is expected between B-Q, Q-S, as well as B-S. On the other hand, in the hadronic sector presence of baryons and mesons would generate an entirely different type of correlations between these quantities. Hence, these correlations are expected to show changes across the phase transition, which are characteristics of the changes in the relevant degrees of freedom.

Correlation functions, $\chi^{ij}_{xx'}$, are defined by

$$\chi^{ij}_{xx'} = \frac{1}{VT^3}\frac{\partial^{i+j}(lnZ)}{\left[\partial\left(\frac{\mu_x}{T}\right)^i\right]\left[\partial\left(\frac{\mu_{x'}}{T}\right)^j\right]}, \tag{14}$$

where x and x' correspond to conserved charges B,S,Q, and μ's are chemical potentials of corresponding conserved charges. In this section we show temperature dependence of various correlation functions at $\mu_B = 0$. We also compare our result with LQCD data [24].

Figure 4 shows the variation of correlations between conserved charges with temperature around $\mu_x = \mu_{x'} = 0$. Since

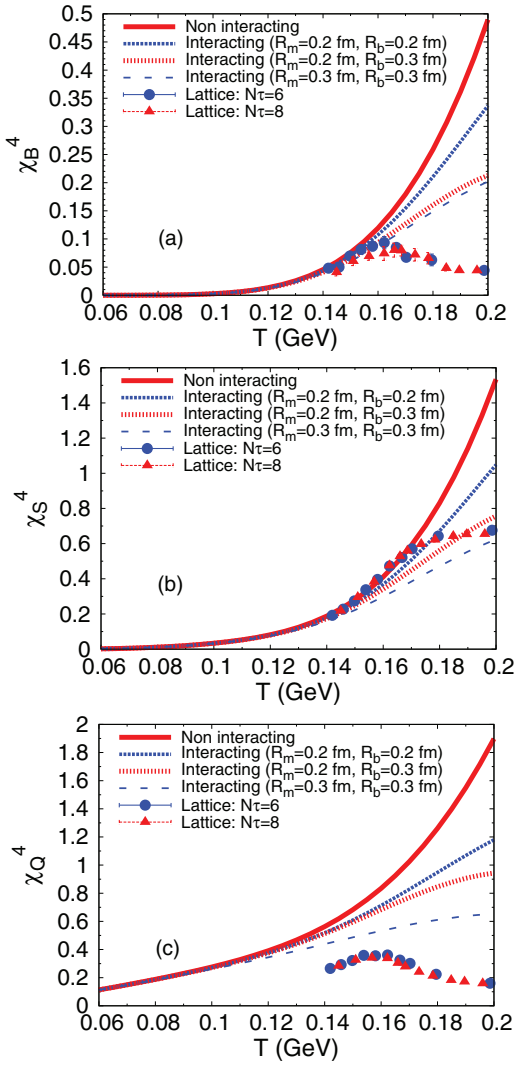

FIG. 3. (Color online) Variation of fourth-order susceptibilities χ_B^4, χ_S^4, χ_Q^4 with temperature ($\mu = 0$). Lattice data is taken from Ref. [72].

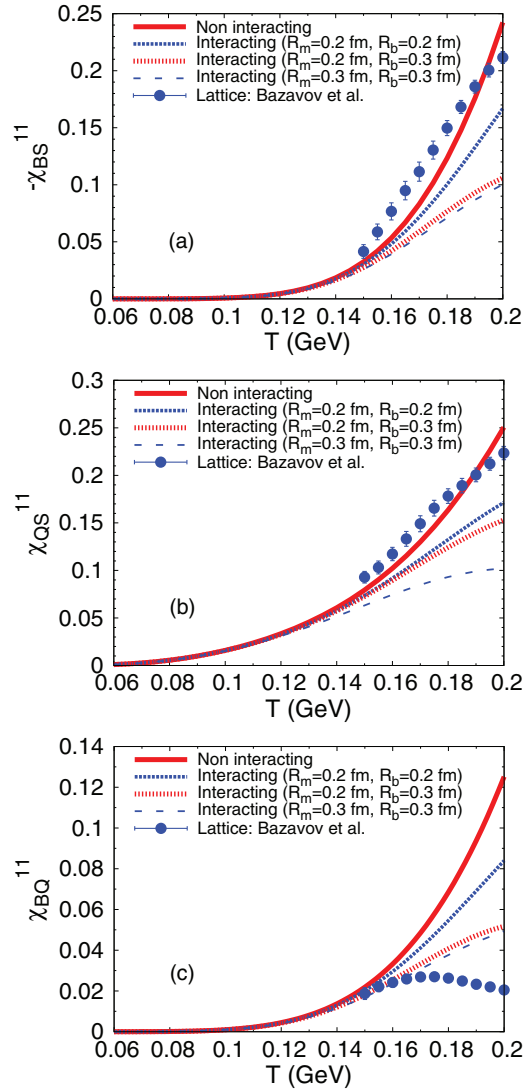

FIG. 4. (Color online) Variation of χ_{BS}^{11}, χ_{BQ}^{11}, and χ_{QS}^{11} with temperature at $\mu = 0$. Lattice data for continuum extrapolation is taken from Ref. [24].

at very low temperature the main contribution comes from pions (baryon number as well as strange quantum number = 0), all the correlations remain zero. The next particle to be excited is kaon and as a result χ_{QS}^{11} becomes nonzero around $T = 0.075$ GeV. The leading contribution to χ_{QS}^{11} in the hadronic sector is due to charge kaons, which has the same sign for charge and strange quantum number. So it remains positive and increases with temperature. Other correlations pick up nonzero values above $T = 0.1$ GeV when baryons start populating the system. χ_{BS}^{11} is proportional to the product of baryon number and strange quantum number. So here most of the contribution is due to lightest baryon Λ which has baryon number $+1$ and strange quantum number -1. Other contributing particles, such as, Σ, Ξ, etc., also have relative negative sign between baryon number and strange quantum number. As a result χ_{BS}^{11} remains negative. This negative value increases with T due to the increase in the population of the strange baryons. Again, HRG results show a sharp increase compared to those from the EVHRG model. Due to the contribution from mesons (mainly kaons) in χ_{QS}^{11}, the meson radius plays a dominating role and an increase in meson radius produces larger suppression in the EVHRG model. On the other hand, baryon radius plays a major role for both χ_{BS}^{11} as well as χ_{BQ}^{11}. The dominant contribution in χ_{BQ}^{11} at low temperature is due to the proton and antiproton and for both of those baryon numbers as well as charge carry the same sign. So the value of χ_{BQ}^{11} remains positive and shows a sharp increase with temperature in HRG, EVHRG being suppressed due to the effect of hard-core radius. In the quark sector strange quarks (antiquarks) carry $1/3$ ($-1/3$) baryon number and the relative sign between B and S is always negative. As a result the lattice result for χ_{BS}^{11} shows a similar trend as that of HRG. On the other hand, χ_{QS}^{11} is always positive as charge as well as strangeness for strange quark is negative. Though the lattice values at lower temperature (0.15 GeV) are close to HRG and EVHRG, χ_{BS}^{11} as well χ_{QS}^{11} for lattice increase

faster than those for HRG as strange quark mass is much smaller compared to strange baryons. At high temperature quark masses decrease (which will eventually become zero at Stefan-Boltzmann limit) and lattice results would start saturating whereas HRG results would keep on increasing. As a result lattice values are suppressed compared to HRG values both for χ^{11}_{QS} and χ^{11}_{BS}. In the case of χ^{11}_{BQ}, EVHRG ($R_m = 0.2$ fm and $R_b = 0.3$ fm) results agree well with the lattice data for $T < 0.17$ GeV. But at higher temperatures, the weighted sum of charges of massless quarks vanishes so the lattice results would start saturating with the further increase in temperature whereas HRG results would keep on increasing similar like χ^{11}_{QS} and χ^{11}_{BS}.

The LQCD results of charge correlations has been found to deviate from the ideal gas limit even at twice the transition temperature and the large contributions of flavor fluctuations are expected to be the cause of these deviations [24]. In order to analyze the experimental results, suitable ratios have been proposed to eliminate these contributions [75]. Three ratios, namely, baryon-strangeness correlation coefficient C_{BS} [75], electric charge-strangeness correlation coefficient C_{QS}, and baryon-electric charge correlation coefficient C_{BQ} can be written as [24]

$$C_{BS} = -3\frac{\chi^{11}_{BS}}{\chi^2_S}, \quad C_{QS} = 3\frac{\chi^{11}_{QS}}{\chi^2_S}, \quad C_{BQ} = \frac{\chi^{11}_{BQ}}{\chi^2_B}. \qquad (15)$$

Figure 5, shows variation of C_{BS}, C_{QS}, and C_{BQ} with temperature at $\mu = 0$. We compare our result with LQCD data [24]. At low temperature C_{BS} is much lower than one because the denominator contains mostly kaons whereas contribution to numerator comes from baryons, mostly Λ, which is less populated than kaons. It increases with temperature but remains below 1 due to larger contribution from mesons. If all the hadronic radii are the same, the interaction effect gets canceled. On the other hand, for larger baryonic radii, the baryon population gets suppressed and C_{BS} value for EVHRG becomes lower than HRG. In case of simple QGP, or more generally, for a system where the quark flavors are uncorrelated, this value will be unity. Since lattice χ^{11}_{BS} is higher, lattice C_{BS} values remain above the HRG (and EVHRG) and saturates at high temperature.

At very low temperature, the contribution to the numerator of C_{QS} come from charged kaons only while the contributions to the denominator come from all the kaons. So C_{QS} comes out to be around 1.5. With increase of temperature λ starts populating the system and C_{QS} becomes close to 1. There is no effect of interaction in most of the temperature range except at very high temperatures. Here, a higher baryonic radii (compared to meson radii) induces a small increase in C_{QS}. Interaction effects get canceled if radii are same for all hadrons. C_{BS} and C_{QS} are related through the equation $C_{QS} = 0.5(3 - C_{BS})$ [24]. So in lattice studies [24] at low temperature, where C_{BS} is very small C_{QS} is near 1.5, same compared to HRG (and EVHRG) and at high temperature tends to one.

At low temperatures, contribution to the numerator of C_{BQ} comes from protons only while the contributions to the denominator come from both protons and neutrons. As a result C_{BQ} is close to 0.5. It decreases slowly with increase in T as

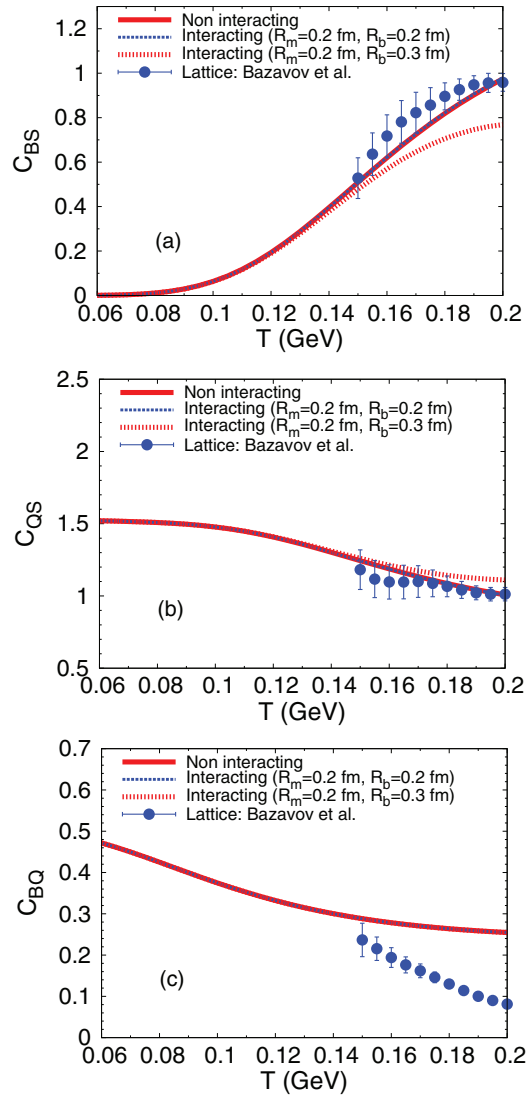

FIG. 5. (Color online) Variation of C_{BS}, C_{QS}, and C_{BQ} with temperature at $\mu = 0$. Lattice data for continuum extrapolation is taken from Ref. [24].

at high T heavier neutral baryons such as Λ start contributing to the denominator whereas only charged baryons contribute to numerator. For both HRG and EVHRG C_{BQ} is very close to each other due to the cancellation of interaction effects. In lattice, C_{BQ} approaches zero at high T as the system is in QGP phase. However at lower temperature it approaches the HRG/EVHRG values.

C. High-density scenario

At very high densities and low temperatures, strongly interacting matter is expected to undergo a first-order phase transition, which ends at CEP as one moves towards higher T and lower μ_B along the phase boundary. At finite μ_B due to the expected stronger divergence at the phase boundary and at CEP, study of higher-order moments is extremely important at finite μ_B. In fact, not only the magnitude but the signs of third moments have also been proposed as a signature for CEP [76].

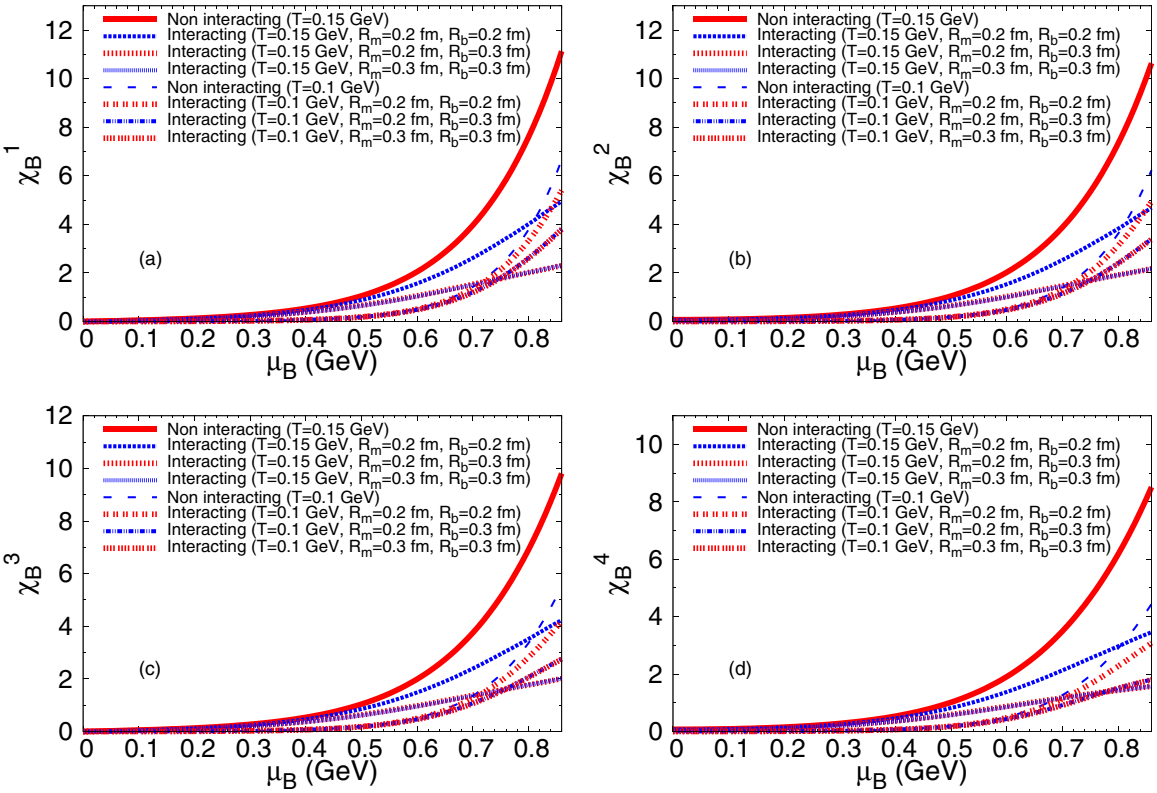

FIG. 6. (Color online) Susceptibilities χ_B^1, χ_B^2, χ_B^3, χ_B^4 as a function of μ_B keeping T fixed and $\mu_S = \mu_Q = 0$.

In this section we have discussed the results of fluctuations and correlations at large μ_B. In Figs. 6–8. we show variation of χ_x^1, χ_x^2, χ_x^3, χ_x^4 with μ_B for a fixed temperature and at $\mu_S = \mu_Q = 0$ where $x = B,S,Q$. Here we have considered $T = 0.1$ GeV and 0.15 GeV for the purpose of illustration. For each temperature we show variation of the quantities with μ_B in the HRG and EVHRG model with different baryon (R_b) and meson (R_m) radii. The effect of interaction is found to be more pronounced at high temperatures. It can be seen from these figures that at high T and large μ_B the magnitude of fluctuations are suppressed by a factor of 2 or more, compared to HRG, if we take the radii of all the hadrons to be 0.2 fm. At high μ_B fluctuations are very sensitive to R_b but not to R_m as in this region system is dominated by baryons. Similar behavior was obtained in Fig. 1 as well. χ_S^1 and χ_S^3 are proportional to the odd power of strange quantum number of the particles. Dominant contribution to χ_S comes from Λ, the lightest strange baryon, which has strange quantum number -1 (at $\mu_S = 0$ strange mesons don't contribute to χ_S^1 and χ_S^3 because particle and antiparticle terms are equal in magnitude but opposite in sign). As a result, χ_S^1 and χ_S^3 remain negative [Figs. 7(a) and 7(c)].

As mentioned earlier, there are contributions from multiple charged hadrons in the electrical charge and strangeness sector only, baryon number being always one. Hence, at high μ_B region magnitudes of χ_x^3 and χ_x^4 are found to be almost double compared to that of χ_x^1 and χ_x^2 respectively for $x = S,Q$ (Figs. 7 and 8), though the change in χ_B remains small as shown in Fig. 6. At very small μ_B and given T (0.1 or 0.15 GeV) system is dominated by mesons and χ_B is small. With increase in μ_B the system will be populated by protons, neutrons, as well as hyperons and χ_B will increase. This increase will be sharper for HRG due to the absence of repulsive interaction.

At finite μ_B (fixed T) due to larger contribution from effective chemical potentials, the effect of interaction, compared to the zero μ_B case, is more prominent on correlations as shown in Fig. 9. The plots are given for different R_m and R_b. It can be seen that at low μ_B, χ_{BS}^{11} and χ_{BQ}^{11} are zero whereas χ_{QS}^{11} is nonzero as pions and kaons are main contributors in this range of parameters. At large μ_B, baryons start populating the system and both B-S and B-Q correlations increase more sharply compared to χ_{QS} as kaons remain the main contributor in χ_{QS} and charge hyperon population is much smaller. One can also see that there is no effect of interaction till $\mu_B = 0.3$ GeV in χ_{BS}^{11} and χ_{BQ}^{11}. However at high T, χ_{QS}^{11} is affected by interaction even at low μ_B.

In Fig. 10 we show variation of C_{BS}, C_{QS}, and C_{BQ} with μ_B at a fixed T and $\mu_S = \mu_Q = 0$. At low μ_B, kaon population is dominating in the denominator of C_{BS} and it is less than unity. On the other hand increase in μ_B facilitates the strange baryon population and C_{BS} increases with increasing μ_B. Moreover, the effect of large μ_B becomes more pronounced for lower T. So that C_{BS} at $T = 0.1$ GeV is larger than that at $T = 0.15$ GeV for large μ_B (>0.6 GeV). Similarly at low μ_B, C_{QS} is around 1.5 as it gets contribution from mainly charged kaons in the numerator and both charged and neutral kaons in denominator. With increase in μ_B, Λ starts populating the system so that C_{QS} keeps decreasing. Since this effect is more pronounced for larger T, C_{QS} is lower for larger T at large μ_B (>0.7 GeV).

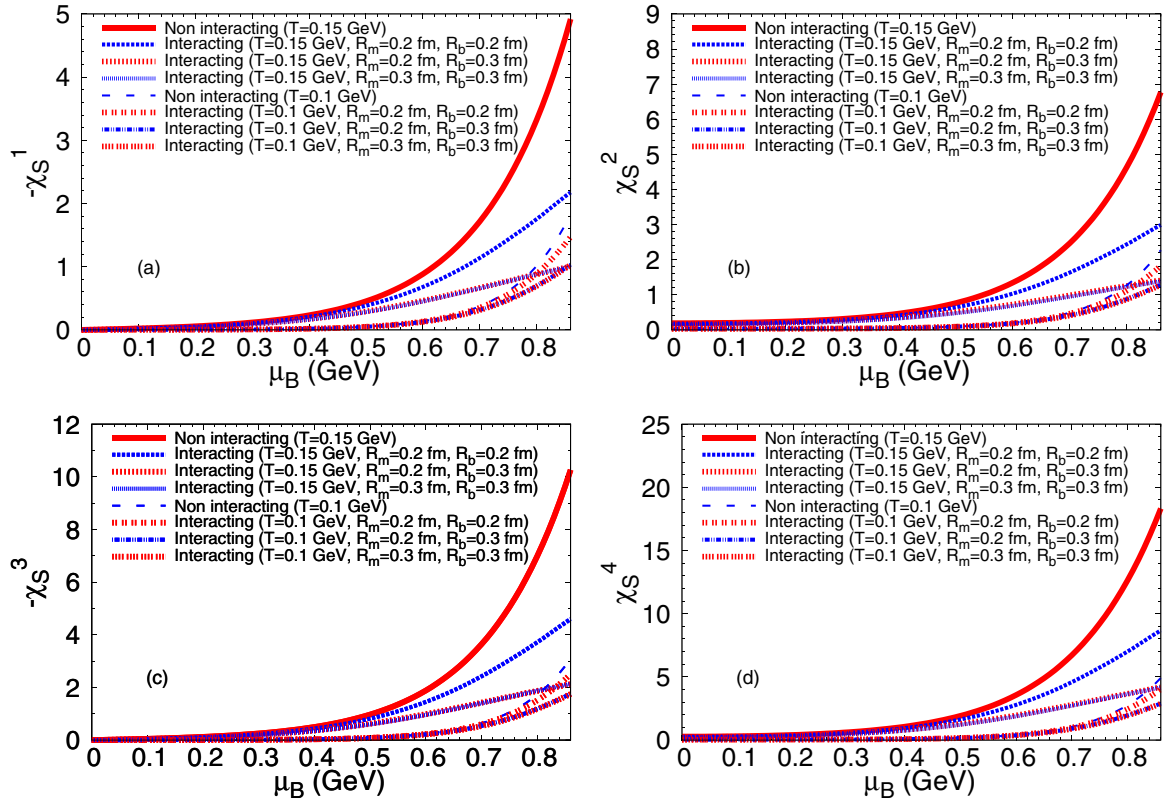

FIG. 7. (Color online) Susceptibilities χ_S^1, χ_S^2, χ_S^3, χ_S^4 as a function of μ_B keeping T fixed and $\mu_S = \mu_Q = 0$.

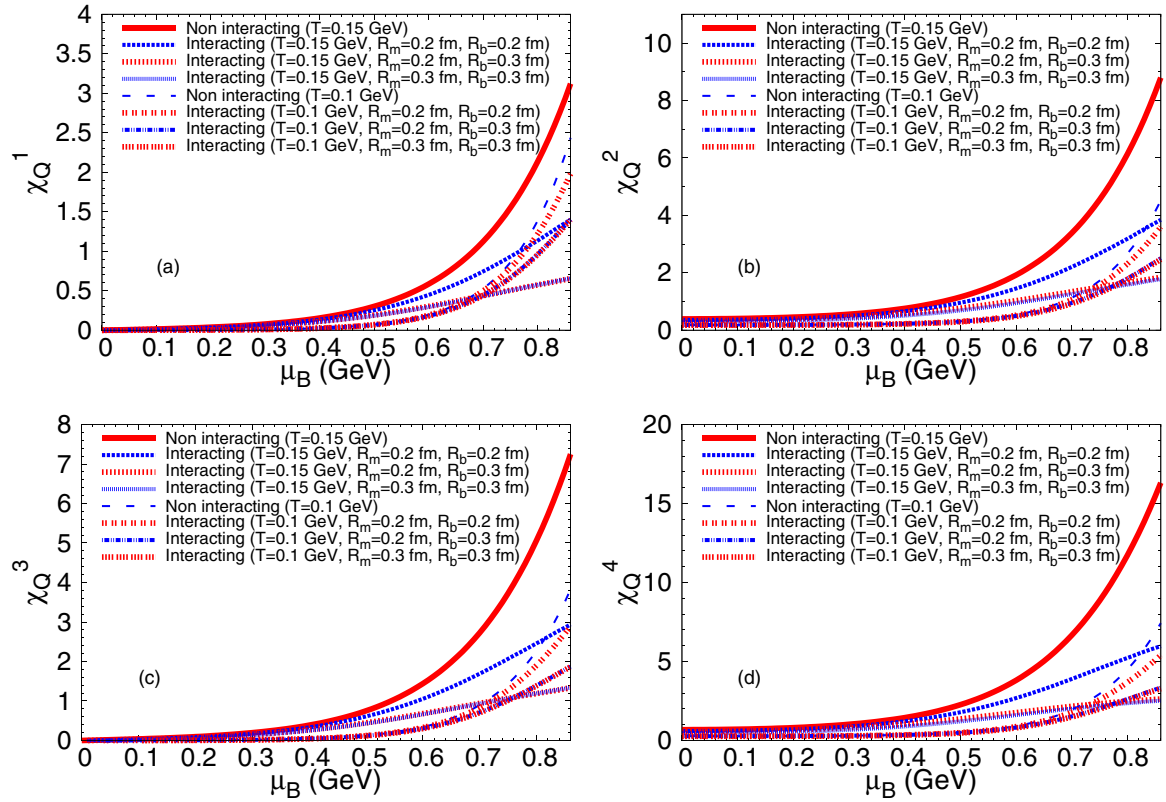

FIG. 8. (Color online) Susceptibilities χ_Q^1, χ_Q^2, χ_Q^3, χ_Q^4 as a function of μ_B keeping T fixed and $\mu_S = \mu_Q = 0$.

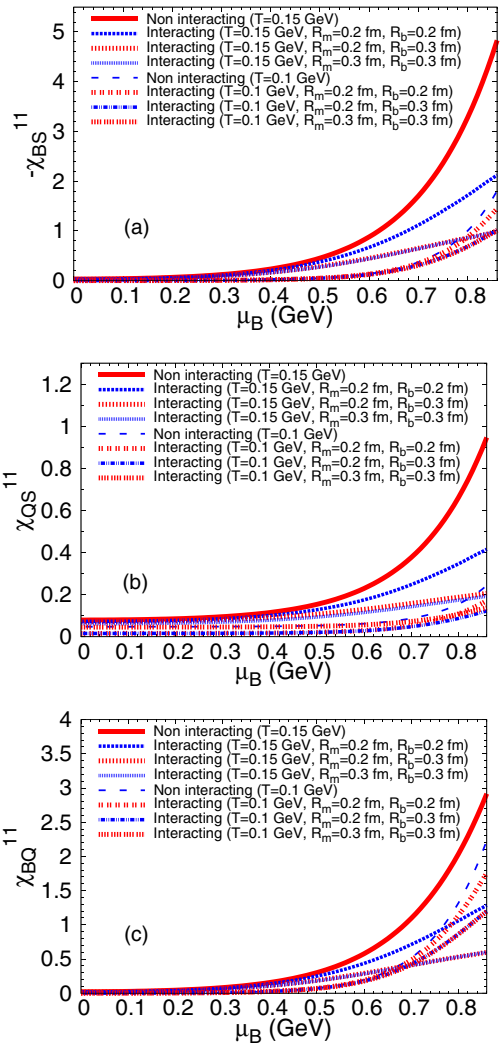

FIG. 9. (Color online) χ^{11}_{BS}, χ^{11}_{BQ}, χ^{11}_{QS} as a function of μ_B keeping $\mu_S = \mu_Q = 0$.

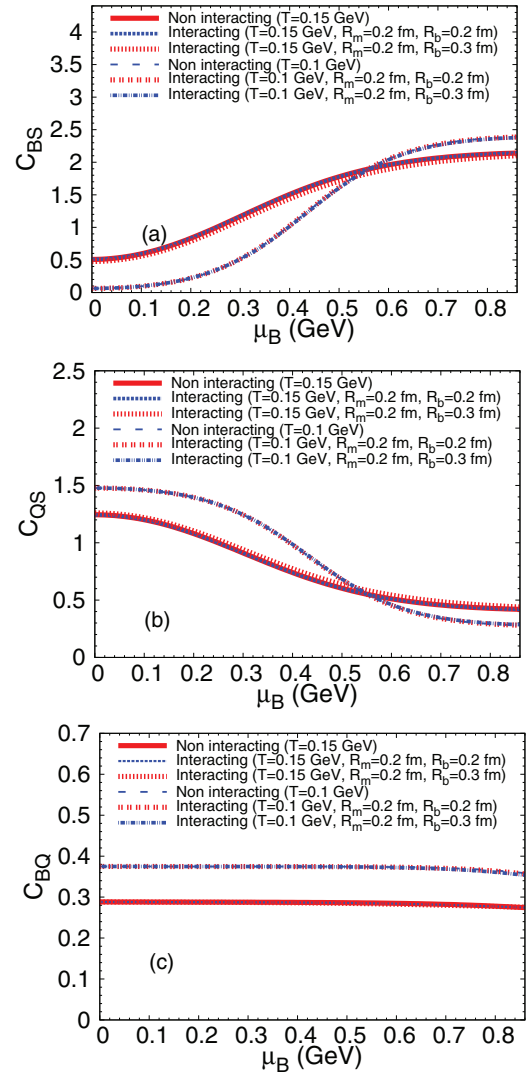

FIG. 10. (Color online) Variation of C_{BS}, C_{QS}, and C_{BQ} with μ_B keeping $\mu_S = \mu_Q = 0$.

At low μ_B, for small T, C_{BQ} gets contribution from protons and neutrons in the denominator and only protons in the numerator. So it is close to 0.5 as shown earlier in Fig. 5(c). At larger T (0.1 or 0.15 GeV), Λ starts contributing in the denominator and C_{BQ} becomes less than 0.5. Similarly as μ_B increases, population of protons, neutrons, and Λ increases. As a result C_{BQ} becomes less than 0.5. At high μ_B, C_{BQ} saturates as rate of increase becomes same for different species. For HRG and EVHRG C_{BQ} is close to each other due to cancellation of interaction effect.

D. Experimental scenario

Experimentally measured moments such as mean (M), standard deviation (σ), skewness (S), and kurtosis (κ) of conserved charges are used to characterize the shape of charge distribution. The standard deviation corresponds to the width of the distribution, the skewness is a measure of the asymmetry of the distribution and kurtosis describes the peakness of the distribution. Products of moments are related to susceptibilities (χ_x) by the following relations,

$$\frac{\chi^2_x}{\chi^1_x} = \frac{\sigma^2_x}{M_x}, \quad \frac{\chi^3_x}{\chi^2_x} = S_x\sigma_x, \quad \frac{\chi^4_x}{\chi^2_x} = \kappa_x\sigma^2_x. \tag{16}$$

The advantage of using the above mentioned products of moments is that they are expected to be independent of the volume of the system. On the other hand, our discussion on the variation of χ_x with T (or μ_B) shows that the cancellation of the volume effect, depending on the degrees of freedom involved, will become less as one increases the order of susceptibility in the numerator (or denominator). In nucleus-nucleus collision experiments, beam energy ($\sqrt{s_{NN}}$) is varied to scan the phase plane. At a particular $\sqrt{s_{NN}}$, if CEP is reached, the signature of CEP could survive during the time evolution of the system. Hence along the freeze-out line one would expect a nonmonotonic behavior of the quantities given in Eq. (16) [62,77]. To compare the products of moments with experiment one has to know freeze-out T and μ at a particular $\sqrt{s_{NN}}$. The freeze-out curve $T(\mu_B)$ can be parametrized

TABLE I. Parametrization of chemical potentials μ_x along the freeze-out curve.

x	d_x (GeV)	e_x (GeV^{-1})
B	1.308 ± 0.028	0.273 ± 0.008
S	0.214	0.161
Q	-0.0211	0.106

by [78]

$$T(\mu_B) = a - b\mu_B^2 - c\mu_B^4, \tag{17}$$

where $a = 0.166 \pm 0.002$ GeV, $b = 0.139 \pm 0.016$ GeV^{-1}, $c = 0.053 \pm 0.021$ GeV^{-3}. The energy dependence of the μ_q can be parametrized as [61]

$$\mu_x(\sqrt{s_{NN}}) = \frac{d_x}{1 + e_x\sqrt{s_{NN}}}, \tag{18}$$

where d_x and e_x are listed in Table I.

The T-μ_B parametrization with $\sqrt{s_{NN}}$ is obtained by fitting the different particle ratios obtained experimentally at different $\sqrt{s_{NN}}$. So for the EVHRG model, in general, the parameters are expected to be different for different hadronic radii. In our study, considering all the particle ratios, we found the parameters to be same as Ref. [78] for $R_b = R_m$. On the other hand, for $R_B \neq R_m$ case, for the radii used here, the parameters are found to be within $\pm 0.005 - 0.008$ GeV of the above fit. Moreover, phenomenological freeze-out condition of fixed energy per nucleon about 1 GeV, calculated in our model, matches quite well with the above mentioned freeze-out parametrization. Hence we have used the above mentioned freeze-out parametrization for comparison with the experimental results. It may also be noted here that as $\sqrt{s_{NN}}$ increases from 7.7 GeV to 200 GeV, T increases from around 0.140 GeV to 0.166 GeV and corresponding μ_B varies between 0.421 GeV to 0.023 GeV. Corresponding μ_S and μ_Q are expected to vary between 0.095 GeV to 0.006 GeV and -0.011 GeV to -0.001 GeV [61].

In terms of transverse momentum (p_T) and rapidity (y) and azimuthal angle (ϕ) d^3p and E_i can be written as $d^3p = p_T\, m_{Ti} \cosh y\, dp_T\, dy\, d\phi$ and $E_i = m_{Ti} \cosh y$, where $m_{Ti} = \sqrt{(p_T^2 + m_i^2)}$. One can write a similar expression in terms of p_T and pseudorapidity η as well. These prescriptions have been used to set the momentum and rapidity acceptance range to compare the present results with the experimental data.

In Fig. 11 we have shown energy dependence of σ^2/M, $S\sigma$, and $\kappa\sigma^2$ for net proton. We compare our result with experimental data of net-proton fluctuations for $(0-5)\%$ central Au-Au collisions measured at STAR [79]. Experimental data is measured at midrapidity ($|y| < 0.5$) and within the transverse momentum range $0.4 < p_T < 0.8$ GeV. Same acceptances range has been used for different hadronic radii in the present manuscript. At low energy, σ^2/M is almost unity and its value increases with increase of $\sqrt{s_{NN}}$ as can be seen from Fig. 11(a). Both the HRG and EVHRG model give almost same result irrespective of the value of radii. At low energy $S\sigma$ for HRG is almost unity and its value decreases with increase of $\sqrt{s_{NN}}$ as can be seen from Fig. 11(b). At low $\sqrt{s_{NN}}$, $S\sigma$ for EVHRG

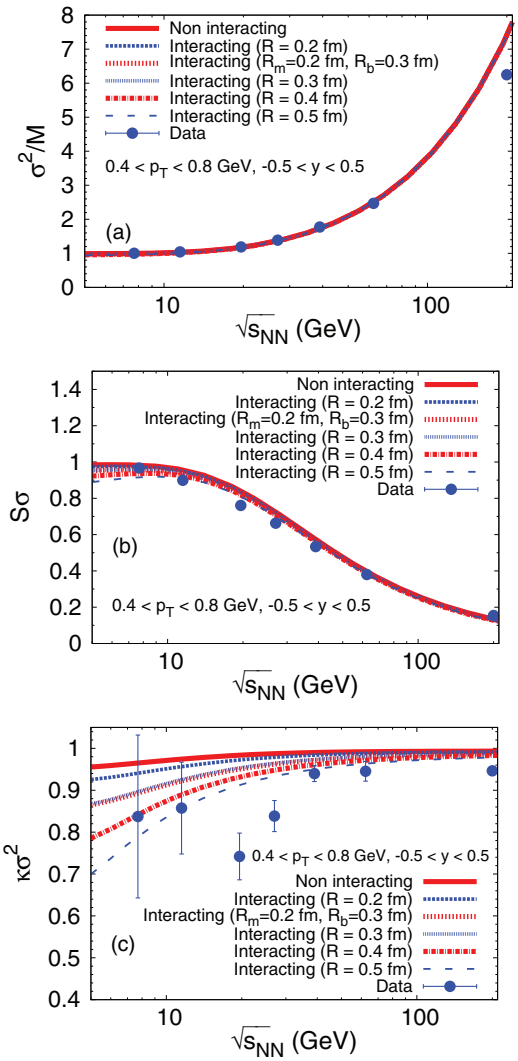

FIG. 11. (Color online) Energy dependence of σ^2/M, $S\sigma$, and $\kappa\sigma^2$ for net proton. Experimental data is taken from Ref. [79].

is less than that of HRG model and suppression increases with increase of radii. However, at high $\sqrt{s_{NN}}$, both HRG and EVHRG model give almost same result. Experimental data of $S\sigma$ can be described well with the EVHRG model for radii of hadrons between 0.3–0.4 fm. At low energy $\kappa\sigma^2$ [Fig. 11(c)] in the HRG model is slightly less than unity and its value reaches to unity as we move to high energy. There is prominent suppression of $\kappa\sigma^2$ in the EVHRG model at low $\sqrt{s_{NN}}$. The $\kappa\sigma^2$ of net proton matches within an error bar with the EVHRG model at $\sqrt{s_{NN}} \geqslant 39$ GeV and $\sqrt{s_{NN}} \leqslant 11.5$ GeV but at intermediate energies EVHRG model overestimates the experimental data. Deviation of experimental data of $S\sigma$ and $\kappa\sigma^2$ for net proton at intermediate energies ($\sqrt{s_{NN}} = 19$ GeV and 27 GeV) may be an indication of existence of quark degrees of freedom or different physics process which is not included in the HRG/EVHRG model.

In Ref. [53], STAR data for net-proton fluctuations is already compared with the EVHRG model in full space. Energy dependence of fluctuations for net proton using LQCD can be found in Refs. [80,81]. Though at high energies, where

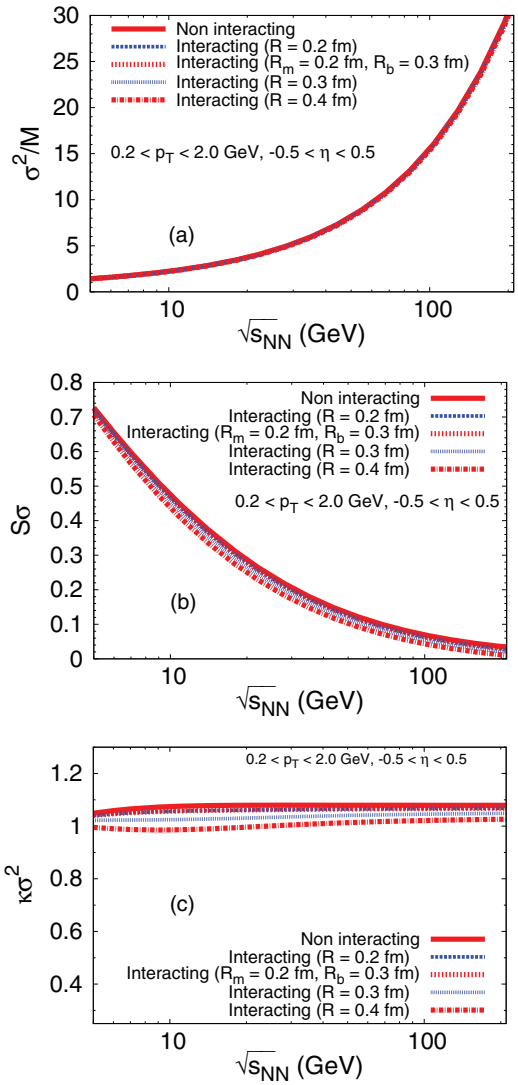

FIG. 12. (Color online) Energy dependence of σ^2/M, $S\sigma$, and $\kappa\sigma^2$ for net kaon.

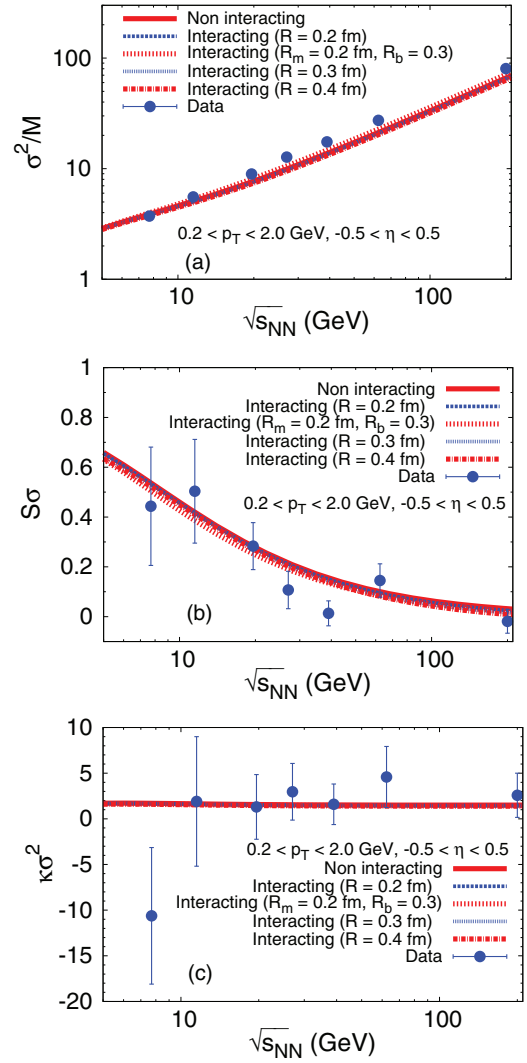

FIG. 13. (Color online) Energy dependence of σ^2/M, $S\sigma$, and $\kappa\sigma^2$ for net charge. Experimental data is taken from Ref. [82].

μ_B is small, LQCD agrees well with the experimental data, at low energies, i.e., for higher μ_B it fails.

In Fig. 12 we have shown energy dependence of σ^2/M, $S\sigma$, and $\kappa\sigma^2$ for net kaon. We have chosen transverse momentum and pseudorapidity within the range $0.2 < p_T < 2.0$ GeV and $-0.5 < \eta < 0.5$ in our calculation. At low energy σ^2/M for net kaon is slightly more than unity and its value increases rapidly with increase of $\sqrt{s_{NN}}$ and result is almost same for both the HRG and EVHRG model. Radii of hadrons practically have no effect on the results as shown in Fig. 12(a). $S\sigma$ for net kaon decreases with increase of $\sqrt{s_{NN}}$ as can be seen from Fig. 12(b). Value of $S\sigma$ in the EVHRG model is suppressed compared to the HRG model and suppression increases with increase of radii of hadrons. In Fig. 12(c) energy dependence of $\kappa\sigma^2$ for net kaon is shown. In this case, volume effect is more prominent, as discussed earlier. $\kappa\sigma^2$ for net kaon increases with increase of $\sqrt{s_{NN}}$ and then saturates. The value of $\kappa\sigma^2$ is suppressed in the EVHRG model compared to the HRG model and suppression increases with increase of radii of hadrons. At all energies $\kappa\sigma^2$ for net kaon lie between 0.9 to 1.1 in both the HRG and EVHRG.

In Fig. 13 we have shown energy dependence of σ^2/M, $S\sigma$, and $\kappa\sigma^2$ for net charge. We have chosen transverse momentum and pseudorapidity within the range $0.2 < p_T < 2.0$ GeV and $-0.5 < \eta < 0.5$ in our model calculation. We have compared our results with experimental data of net-charge fluctuations for (0−5)% central Au-Au collisions measured at STAR [82]. Figure 13(a) shows σ^2/M, for net charge, increases rapidly with increase of $\sqrt{s_{NN}}$ and compared to experimental values our results are suppressed at higher energies. $S\sigma$ for net charge decreases with increase of $\sqrt{s_{NN}}$ as can be seen from Fig. 13(b). Experimental data of $S\sigma$ for net charge matches within an error bar with the HRG/EVHRG model at $\sqrt{s_{NN}} \leqslant 19.6$ GeV and $\sqrt{s_{NN}} \geqslant 62.4$ GeV but at other intermediate energies the HRG/EVHRG model over estimate the experimental data. Figure 13(c) shows $\kappa\sigma^2$ for net charge slowly decreases with increase of $\sqrt{s_{NN}}$ and then saturates. At all $\sqrt{s_{NN}}$, $\kappa\sigma^2$ for net charge lies between 1.4–1.8 in both

the HRG and EVHRG model, which is in agreement with experiment within error-bar at $\sqrt{s_{NN}} \geqslant 11.5$ GeV. Calculations for ratios of higher-order fluctuations of electric charge using LQCD can be found in Ref. [83].

IV. DISCUSSION AND CONCLUSION

We have shown fluctuations (χ_x^i; $i = 1-4; x = B,S,Q$) of various conserved charges such as net baryon number, net strangeness, and net charge at finite temperatures and chemical potentials using interacting and noninteracting hadron resonance gas model and compared them with the lattice as well as experimental data.

We can draw following inferences from the present study.

(i) In general HRG results are larger compared to EVHRG, the difference being higher for higher temperatures and densities.

(ii) At high temperatures and $\mu_B = 0$, compared to HRG, second-order fluctuations from EVHRG fits better to LQCD continuum data for radius of hadrons between 0.2–0.3 fm.

(iii) The LQCD data ($N_\tau = 6,8$) for χ_B^4 and χ_S^4 are in good agreement with the HRG/EVHRG model up to $T = 0.16$ GeV. Whereas, both the HRG and EVHRG model overestimate LQCD data for χ_Q^4.

(iv) Correlations at $T \neq 0$ and $\mu_B = 0$ shows much stronger dependence on the degrees of freedom involved. Lattice continuum data for both χ_{BS}^{11} and χ_{QS}^{11} are closer to HRG results (higher than EVHRG) at lower T but rises less sharply and becomes less than HRG for higher T. On the other hand, χ_{BQ}^{11} calculated in lattice is close to EVHRG results at lower T. Initially it increases with T but then decreases beyond $T = 0.165$ GeV as discussed earlier.

(v) The correlation ratios from both HRG and EVHRG disagree with LQCD continuum data though the trends are qualitatively similar. This difference could be attributed to the fact that LQCD incorporates transition from hadronic to quark degrees of freedom, whereas only hadronic degrees of freedom are present in the HRG or EVHRG model. At high μ_B, the magnitudes of susceptibilities as well as correlations are higher correspond to $\mu = 0$ case.

(vi) The susceptibilities as well as correlations are found to increase with μ_B at fixed temperatures for both HRG and EVHRG, the effect of interaction being larger for higher T.

(vii) Since low-energy collisions usually correspond to larger μ_B, the effect of repulsive interaction, as present in EVHRG, is distinguishable for lower energies. Moreover this difference is more pronounced for higher-order susceptibilities.

(viii) With increase of $\sqrt{s_{NN}}$, chemical potential decreases sharply whereas temperature increases slowly. Therefore, χ^1 and χ^3 decrease with increase of $\sqrt{s_{NN}}$ whereas χ^2 and χ^4 decrease slowly and then saturate. As a result σ^2/M increases with increase of $\sqrt{s_{NN}}$, $S\sigma$ decreases with increase of $\sqrt{s_{NN}}$ whereas $\kappa\sigma^2$ remains almost constant in all energies.

(ix) Although the variations of σ^2/M and $S\sigma$ with $\sqrt{s_{NN}}$ seem to describe the experimental data well, higher moment $\kappa\sigma^2$ shows large deviations. It may be an indication of quark degrees of freedom. It would be interesting to look at the other higher moments as they are supposed to have stronger dependence on correlation length and hence will be more sensitive to the critical fluctuations.

In general, EVHRG seems to have a better agreement with the LQCD continuum data at low T and $\mu_B = 0$. But the comparison with the experimental data does not provide us with a clear preference between HRG and EVHRG.

It may be noted that in Figs. 2(c) and 4(a) LQCD results are larger than all the HRG results in the crossover temperature range of 0.14–0.15 GeV. The LQCD may become closer to the HRG by the inclusion of non-PDG additional strange beryons which, though not observed experimentally, are predicted by the quark model and also observed in the LQCD spectrum [84].

Here we would like to mention that the grand canonical (GC) description as used for the present study is usually considered as the relevant description for the systems in heavy-ion collision [85]. But if the conserved quanta under consideration is small then one needs to take care of the charge conservations and the present description will not be appropriate. More specifically, it has been found that the results for scaled variances vary for different ensembles though the mean multiplicities from different ensembles tend to agree with each other in the infinite volume limit [86]. Moreover, the microcanonical ensemble seems to give a better agreement with the data [86]. These findings definitely suggest the importance of the conservation laws. We plan to study these aspects in our future work.

ACKNOWLEDGMENTS

The work is funded by CSIR, UGC (DRS) and DST of the Government of India. The authors thank the STAR Collaboration for providing the experimental data. We would like to thank Anirban Lahiri, Sarbani Majumder, Xiaofeng Luo, Nihar Ranjan Sahoo, and Swagato Mukherjee for useful discussions.

[1] Y. Aoki, G. Endrodi, Z. Fodor, S. D. Katz, and K. K. Szabo, Nature (London) **443**, 675 (2006).
[2] F. R. Brown *et al.*, Phys. Rev. Lett. **65**, 2491 (1990).
[3] S. Ejiri, Phys. Rev. D **78**, 074507 (2008).
[4] R. D. Pisarski and F. Wilczek, Phys. Rev. D **29**, 338 (1984).
[5] M. Asakawa and K. Yazaki, Nucl. Phys. A **504**, 668 (1989).
[6] M. A. Halasz, A. D. Jackson, R. E. Shrock, M. A. Stephanov, and J. J. M. Verbaarschot, Phys. Rev. D **58**, 096007 (1998).

[7] Y. Hatta and T. Ikeda, Phys. Rev. D **67**, 014028 (2003).
[8] E. S. Bowman and J. I. Kapusta, Phys. Rev. C **79**, 015202 (2009).
[9] Z. Fodor and S. D. Katz, J. High Energy Phys. 04 (2004) 050.
[10] M. A. Stephanov, Prog. Theor. Phys. Suppl. **153**, 139 (2004).
[11] R. V. Gavai and S. Gupta, Phys. Rev. D **71**, 114014 (2005).
[12] B.-J. Schaefer and J. Wambach, Phys. Rev. D **75**, 085015 (2007).
[13] R. V. Gavai and S. Gupta, Phys. Rev. D **78**, 114503 (2008).
[14] M. Cheng *et al.*, Phys. Rev. D **79**, 074505 (2009).
[15] G. Boyd, J. Engels, F. Karsch, E. Laermann, C. Legeland, M. Lugermeier, and B. Peterson, Nucl. Phys. B **469**, 419 (1996).
[16] J. Engels, O. Kaczmarek, F. Karsch, and E. Laermann, Nucl. Phys. B **558**, 307 (1999).
[17] Z. Fodor and S. D. Katz, Phys. Lett. B **534**, 87 (2002).
[18] Z. Fodor, S. D. Katz, and K. K. Szabo, Phys. Lett. B **568**, 73 (2003).
[19] C. R. Allton, S. Ejiri, S. J. Hands, O. Kaczmarek, F. Karsch, E. Laermann, Ch. Schmidt, and L. Scorzato, Phys. Rev. D **66**, 074507 (2002).
[20] C. R. Allton, S. Ejiri, S. J. Hands, O. Kaczmarek, F. Karsch, E. Laermann, and Ch. Schmidt, Phys. Rev. D **68**, 014507 (2003).
[21] C. R. Allton, M. Doring, S. Ejiri, S. J. Hands, O. Kaczmarek, F. Karsch, E. Laermann, and K. Redlich, Phys. Rev. D **71**, 054508 (2005).
[22] P. de Forcrand and O. Philipsen, Nucl. Phys. B **642**, 290 (2002); **673**, 170 (2003).
[23] Y. Aoki, Z. Fodor, S. D. Katz, and K. K. Szabo, Phys. Lett. B **643**, 46 (2006).
[24] A. Bazavov *et al.*, Phys. Rev. D **86**, 034509 (2012).
[25] S. Borsányi *et al.*, J. High Energy Phys. 11 (2010) 077.
[26] M. Cheng *et al.*, Phys. Rev. D **77**, 014511 (2008).
[27] S. Borsányi *et al.*, J. High Energy Phys. 1201 (2012) 138.
[28] P. N. Meisinger and M. C. Ogilvie, Phys. Lett. B **379**, 163 (1996); Nucl. Phys. B (Proc. Suppl.) **47**, 519 (1996); K. Fukushima, Phys. Lett. B **591**, 277 (2004); E. Megías, E. R. Arriola, and L. L. Salcedo, Phys. Rev. D **74**, 065005 (2006); E. Megias, E. R. Arriola, and L. L. Salcedo, *ibid.* **74**, 114014 (2006); J. High Energy Phys. 01 (2006) 073; C. Ratti, M. A. Thaler, and W. Weise, Phys. Rev. D **73**, 014019 (2006); S. K. Ghosh, T. K. Mukherjee, M. G. Mustafa, and R. Ray, *ibid.* **73**, 114007 (2006).
[29] S. Mukherjee, M. G. Mustafa, and R. Ray, Phys. Rev. D **75**, 094015 (2007); S. K. Ghosh, T. K. Mukherjee, M. G. Mustafa, and R. Ray, *ibid.* **77**, 094024 (2008); A. Bhattacharyya, P. Deb, A. Lahiri, and R. Ray, *ibid.* **82**, 114028 (2010); **83**, 014011 (2011).
[30] M. A. Stephanov, Phys. Rev. Lett. **102**, 032301 (2009).
[31] P. Braun-Munzinger, K. Redlich, and J. Stachel, in *Quark Gluon Plasma 3*, edited by R. C. Hwa and X. N. Wang (World Scientific, Singapore, 2004).
[32] P. Braun-Munzinger, J. Stachel, J. P. Wessels, and N. Xu, Phys. Lett. B **344**, 43 (1995).
[33] J. Cleymans, D. Elliott, H. Satz, and R. L. Thews, Z. Phys. C **74**, 319 (1997).
[34] P. Braun-Munzinger, I. Heppe, and J. Stachel, Phys. Lett. B **465**, 15 (1999).
[35] J. Cleymans and K. Redlich, Phys. Rev. C **60**, 054908 (1999).
[36] F. Becattini, J. Manninen, M. Gaździcki, Phys. Rev. C **73**, 044905 (2006).
[37] P. Braun-Munzinger, D. Magestro, K. Redlich, and J. Stachel, Phys. Lett. B **518**, 41 (2001).
[38] A. Andronic, P. Braun-Munzinger, and J. Stachel, Nucl. Phys. A **772**, 167 (2006).
[39] A. Andronic, P. Braun-Munzinger, and J. Stachel, Phys. Lett. B **673**, 142 (2009).
[40] S. Gottlieb, W. Liu, D. Toussaint, R. L. Renken, and R. L. Sugar, Phys. Rev Lett. **59**, 2247 (1987).
[41] R. V. Gavai, S. Gupta, and P. Majumdar, Phys. Rev. D **65**, 054506 (2002).
[42] C. Bernard *et al.*, Phys. Rev. D **71**, 034504 (2005).
[43] C. Bernard *et al.*, Phys. Rev. D **77**, 014503 (2008).
[44] R. Hagedorn and J. Rafelski, Phys. Lett. B **97**, 136 (1980).
[45] D. H. Rischke, M. I. Gorenstein, H. Stöcker, and W. Greiner, Z. Phys. C **51**, 485 (1991).
[46] J. Cleymans, M. I. Gorenstein, J. Stalnacke, and E. Suhonen, Phys. Scr. **48**, 277 (1993).
[47] C. P. Singh, B. K. Patra, and K. K. Singh, Phys. Lett. B **387**, 680 (1996).
[48] G. D. Yen, M. I. Gorenstein, W. Greiner, and S. N. Yang, Phys. Rev. C **56**, 2210 (1997).
[49] M. I. Gorenstein, M. Hauer, and O. N. Moroz, Phys. Rev. C **77**, 024911 (2008).
[50] A. Andronic, P. Braun-Munzinger, J. Stachel, and M. Winn, Phys. Lett. B **718**, 80 (2012).
[51] J. Fu, Phys. Rev. C **85**, 064905 (2012).
[52] V. V. Begun, M. Gaździcki, and M. I. Gorenstein, Phys. Rev. C **88**, 024902 (2013).
[53] J. Fu, Phys. Lett. B **722**, 144 (2013).
[54] A. Tawfik, Phys. Rev. C **88**, 035203 (2013).
[55] R. Dashen and S. K. Ma, Phys. Rev. A **4**, 700 (1971).
[56] Y. Hama, T. Kodama, and O. Socolowski, Braz. J. Phys. **35**, 24 (2005).
[57] K. Werner, Iu. Karpenko, T. Pierog, M. Bleicher, and K. Mikhailov, Phys. Rev. C **82**, 044904 (2010).
[58] A. V. Merdeev, L. M. Satarov, and I. N. Mishustin, Phys. Rev. C **84**, 014907 (2011).
[59] P. Garg, D. K. Mishra, P. K. Netrakanti, B. Mohanty, A. K. Mohanty, B. K. Singh, and N. Xu, Phys. Lett. B **726**, 691 (2013).
[60] S. Ejiri, F. Karsch, and K. Redlich, Phys. Lett. B **633**, 275 (2006).
[61] F. Karsch and K. Redlich, Phys. Lett. B **695**, 136 (2011).
[62] M. M. Aggarwal *et al.* (STAR Collaboration), Phys. Rev. Lett. **105**, 022302 (2010).
[63] K. Nakamura *et al.* (Particle Data Group), J. Phys. G: Nucl. Part. Phys. **37**, 075021 (2010).
[64] S. R. Amendolia *et al.*, Nucl. Phys. B **277**, 168 (1986); Phys. Lett. B **178**, 435 (1986); G. Simon, C. Schmitt, F. Borkowski, and V. Walther, Nucl. Phys. A **333**, 381 (1980); T. Udem, A. Huber, B. Gross, J. Reichert, M. Prevedelli, M. Weitz, and T. W. Hänsch, Phys. Rev. Lett. **79**, 2646 (1997); P. Mergell, U. G. Meissner, and D. Drechsel, Nucl. Phys. A **596**, 367 (1996).
[65] B. Povh and J. Hüffner, Phys. Rev. Lett. **58**, 1612 (1987); J. Hüffner and B. Povh, Phys. Lett. B **215**, 772 (1988).
[66] A. Bohr and B. Mottelson, in *Nuclear Structure* (Benjamin, New York, 1969), Vol. 1, p. 266.
[67] D. A. Giltinan and R. M. Thaler, Phys. Rev. **131**, 805 (1963).
[68] M. Asakawa, U. Heinz, and B. Müller, Phys. Rev. Lett. **85**, 2072 (2000).
[69] D. Bower and S. Gavin, Phys. Rev. C **64**, 051902 (2001).
[70] M. Abdel-Aziz and S. Gavin, Phys. Rev. C **70**, 034905 (2004).
[71] A. Bazavov *et al.*, arXiv:1407.6387v1 [hep-lat].

[72] A. Bazavov *et al.*, Phys. Rev. Lett. **109**, 192302 (2012); C. Schmidt (for the BNL-Bielefeld Collaboration), PoS ConfinementX, 187 (2012); A. Bazavov *et al.*, Phys. Rev. Lett. **111**, 082301 (2013).
[73] P. Huovinen and P. Petreczky, J. Phys.: Conf. Series **230**, 012012 (2010).
[74] S. Borsányi *et al.*, Nucl. Phys. A **855**, 253 (2011).
[75] V. Koch, A. Majumder, and J. Randrup, Phys. Rev. Lett. **95**, 182301 (2005).
[76] M. Asakawa, S. Ejiri, and M. Kitazawa, Phys. Rev. Lett. **103**, 262301 (2009).
[77] A. Tawfik, Adv. High Energy Phys. (2013) 574871.
[78] J. Cleymans, H. Oeschler, K. Redlich, and S. Wheaton, Phys. Rev. C **73**, 034905 (2006).
[79] X. Luo (for the STAR collaboration), Nucl. Phys. A **904–905**, 911c (2013).
[80] S. Gupta, X. Luo, B. Mohanty, H.-G. Ritter, and Nu Xu, Science **332**, 1525 (2011).
[81] F. Karsch and K. Redlich, Phys. Rev. D **84**, 051504(R) (2011).
[82] L. Adamczyk *et al.* (STAR Collaboration), Phys. Rev. Lett. **113**, 092301 (2014).
[83] S. Borsányi, Z. Fodor, S. D. Katz, S. Krieg, C. Ratti, and K. K. Szabo, Phys. Rev. Lett. **111**, 062005 (2013).
[84] A. Bazavov *et al.*, Phys. Rev. Lett. **113**, 072001 (2014).
[85] S. Jeon and V. Koch, in *Quark Gluon Plasma 3*, edited by R. C. Hwa and X. N. Wang (World Scientific, Singapore, 2004), p. 430.
[86] V. V. Begun, M. Gazdźicki, M. I. Gorenstein, M. Hauer, V. P. Konchakovski, and B. Lungwitz, Phys. Rev. C **76**, 024902 (2007) and references therein.